Investigation on machining of a Ti-6Al-4V alloy using FEM Simulation and experimental analysis

M. Sahli[1*], M. Abid[1], T. Barrière[2] and B. Mamen[3]

[1] Normandie Univ, ENSICAEN, UNICAEN, CEA, CNRS, CIMAP, 14000 Caen, France

[2] University Bourgogne-Franche-Comté, COMUE UBFC, Femto-ST Institute, Department of Applied Mechanics, 24 Rue de l'Epitaphe, 25030 Besançon, France

[3]Department of Civil Engineering, Abbès Laghrour University, 40000 Khenchela, Algeria

Abstract

Titanium alloys have been attracting from the more industries, especially, industry aerospace due to their very important high strength to weight ratio. Furthermore, they were classified as difficult to machine materials due to low tool life in machining processes. In this study, a FE model has been developed to simulate the turning stage of Ti-6Al-4V alloy. A 3D model with thermo-mechanical coupling has been proposed to study the influence of cutting parameters and also lubrication on the performance of cutting tools. The constants of the Johnson-Cook constitutive model of Ti-6Al-4V alloy were identified using inverse analysis based on the process parameters of the orthogonal cutting. The predictive FE model has been validated based on an orthogonal cutting test. The investigations indicated that this approach estimates the resultant cutting forces with low prediction errors. Indeed, the predicted forces showed good agreement with the experimental data, with minimum and maximum error magnitudes of 2.8 and 8.7% for cutting force, and 1.3 and 6.8% for feed force, respectively.

Keywords: Titanium turning, cutting tools, FE simulation, chip.

1. Introduction

Metal chip removal machining was frequently used in the mechanical fabrication industry [1-4]. It makes it possible to obtain parts of complex shape characterized by a low roughness of the surface states at a fairly low cost, etc. Some alloys such as super alloys-based Cr, Ni and Ti were machined in a conventional manner and lead to rapid wear of the edges of cutting inserts for their high strength and abrasiveness, even at fairly high cutting speeds. Their low thermal conductivity therefore prevents the dissipation of the heat generated by the cutting, which causes a rapid increase in the heat increase of the workpiece [5-7]. This leads to early damage of the cutting insert and directly affects the final quality of the workpiece and its machined surface [8,9]. Chip formation will affect machining temperature, cutting force, tool life and other cutting process parameters [10,11]. The selection of appropriate cutting parameters therefore essentially improves the surface integrity induced by machining [12]. Vyas and Shaw and Hua and Shivpuri indicate that the titanium alloy chip segmentation was due to a crack initiation companioned by propagation inside the primary shear zone [13,14].

In this context, it was interesting to propose a reliable 3D FE model which allows us a better understanding of the cutting insert-part interaction during the machining of this type of alloys. Numerical simulation of machining process and the residual

stresses induced by the cutting operation have been investigated by many researchers [15-20]. Li et al. have set up an experimental plan to study the effect of machining parameters and the inclination angle of the cutting tool on the chips formation during the machining of the titanium alloy Ti-6Al -4V [10]. Chen et al. performed a numerical study to analyse the high-speed machining of titanium alloy Ti-6Al-4V using the Johnson-Cook material model coupled with a ductile failure criterion to analyse the process parameters effect on machining on the final morphology of the chips [21]. Takahashi et al. studied numerically analysed the effects of the rotational speed of the workpiece on the sense of chip flow and the cutting force of tools during turning process [3]. It was concluded that the machining force significantly reduced by increasing the rotational speed of the tool when the sense of chip flow was tilted towards the direction of the tool rotation. Chen et al. proposed an FE model for machining strain prediction using the finite element method that takes into account the strain during the previous cut and the nominal depth of cut of the current cut [22]. Zhao et al. proposed a 2D model to study the orthogonal cutting of SiCp/2024Al [23]. It was observed that the interaction tool with the elements of the reinforcement was the main reason for the defects observed on the machining surface and the wear of the cutting inserts. The modeling of metal cutting has therefore proved to be particularly complex due to the diversity of the physical phenomena involved, in particular thermomechanical coupling, contact / friction and material rupture. This was because during filming, plastic deformation and friction work were the main sources of heat in the processing area and can significantly increase the temperature in the cutting area. This increase in temperature can significantly affect various mechanical and thermal properties of the material of the part.

In summary, several analytical, FE simulation and experimental methods have been implemented to study the machining of mechanical parts. Researchers mainly focused on developing models of the workpiece-tool machining system and correlating them with machining stability using analytical and finite element methods. Rare were those who have proposed models with thermomechanical coupling for the machining of mechanical parts in Ti-6Al-4V alloy. Therefore, the objective of this work was to develop a 3D FE model with a generalized Johnson-Cook (JC) constitutive law and very realistic initial and boundary conditions to obtain the response adapted to the applied cutting conditions. Such a model would facilitate a closer approximation to the machining knowledge of Ti-6Al-4V alloy parts without performing the machining experiments.

In this study, machining tests of Ti-6Al-4V alloy under starved or full lubrication were performed at different cutting speeds using conventional tools. We also focused on the investigation of the cutting effects on the cutting performance in terms of cutting forces and friction coefficient. Then, 3D model with thermo-mechanical coupling has been proposed to study the influence of cutting parameters on the performance of cutting tools. This model was allowed us on the one hand to study the chip formation and on the other hand, to predict the stresses distributions, cutting forces and temperatures evolutions in the workpiece and the cutting insert.

2. Materials and experimental methods

2.1. Materials

Machining experiments were carried-out on a cylindrical part made of wrought titanium alloy (Ti-6Al-4V) with a diameter of 50 mm and a length of 200 mm. In these tests, cemented carbide cutting inserts supplied by Sandvik Company were used. These GC6050 type inserts with a titanium-aluminum nitride (TiAlN) coating have been tested under different cutting conditions. The physical characteristics of the material to be machined and those of the cutting inserts were shown in Tables 1 and 2.

Proprieties	**Workpiece (Ti6Al4V)**	**Tool (Wc-Co)**
Density	4430	15700
Young's modulus [MPa]	1.13xe5	6.50xe5
Poisson ratio	0.34	0.25
Thermal conductivity [w/(m°C)]	K(T)	91
Specific heat capacity [J/(kg°C)]	C_p(T)	206

Table 1. Material characteristics for the cylindrical bar and the cutting insert used in FE simulations.

Proprieties/Temperature [°C]	0	250	500	750	1000	1250	1500
K(T) [w/(m°C)]	6.651	6.996	8.591	8.591	15.031	19.106	22.286
C_p(T) [J/(kg°C)]	483.3	535.8	588.3	640.8	600.19	645.2	690.2

Table 2. Temperature dependent properties of titanium alloy [24].

2.2. Experimental methods

The cutting effects on machining performance were carried-out on a GILDEMEISTER CTX 320 linear cnc lathe V6 under different cutting conditions and with starved or full lubrication. The cutting experiments were stopped after a cutting length of 100 mm and the chips were collected.

Kistler quartz multicomponent dynamometer (type 9257B) features a measuring range of up to 10 kN was used to measure the cutting force values in the machining experiments. All the tests were carried-out using the following parameters: feed rate f = 0.2 mm/revolution; cutting depth a_p = 0.5 mm; cutting speed of 40-200 m/min.

3. Experimental results and discussion

Figure 1 illustrates the cutting force evolution for textured tools, during the machining phase under conditions lubricated by starved or complete fluid system. It can be observed that the experimental values of the recorded machining force were very stable during the machining phase under complete lubricated conditions.

The same values of the three cutting force components remained constant using starved lubrication in the interval between the first 30 to 40 s; then an increase was observed around 20% to 24% (see Fig.1).

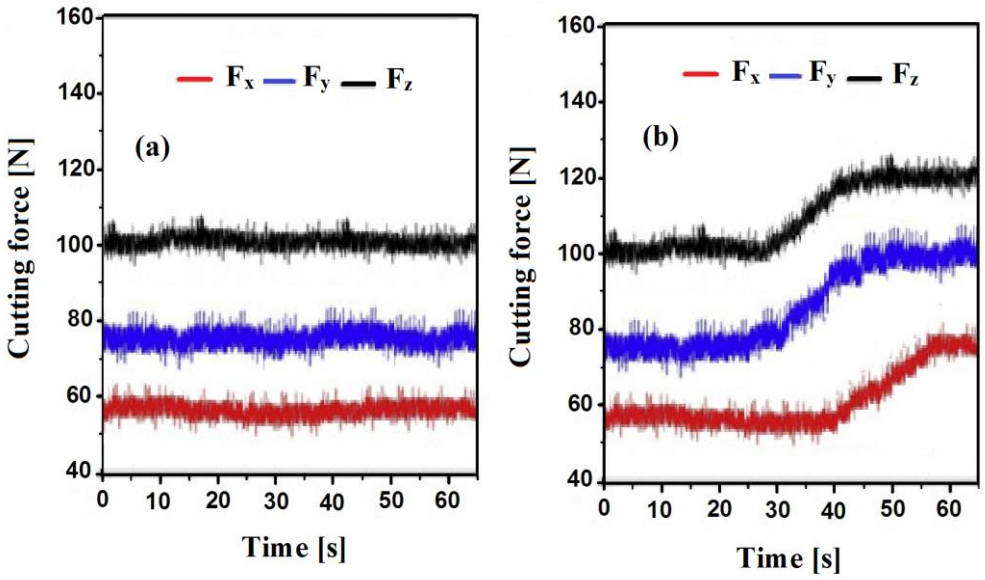

Fig.1. Cutting forces evolution vs. time in textured cutting surface under (a) full lubrication and (b) starved lubrication (cutting velocity: 160 m/min).

Figure 2 shows the friction coefficient evolution as a function of the cutting speed under two lubricated conditions. The results obtained showed that the values of the friction coefficient decreased from 5% to 7% when the cutting speed increased for the machining phase either under complete lubrication or even under insufficient lubrication. It was clear that full lubrication of the cutting tool improves tribological performance a little better.

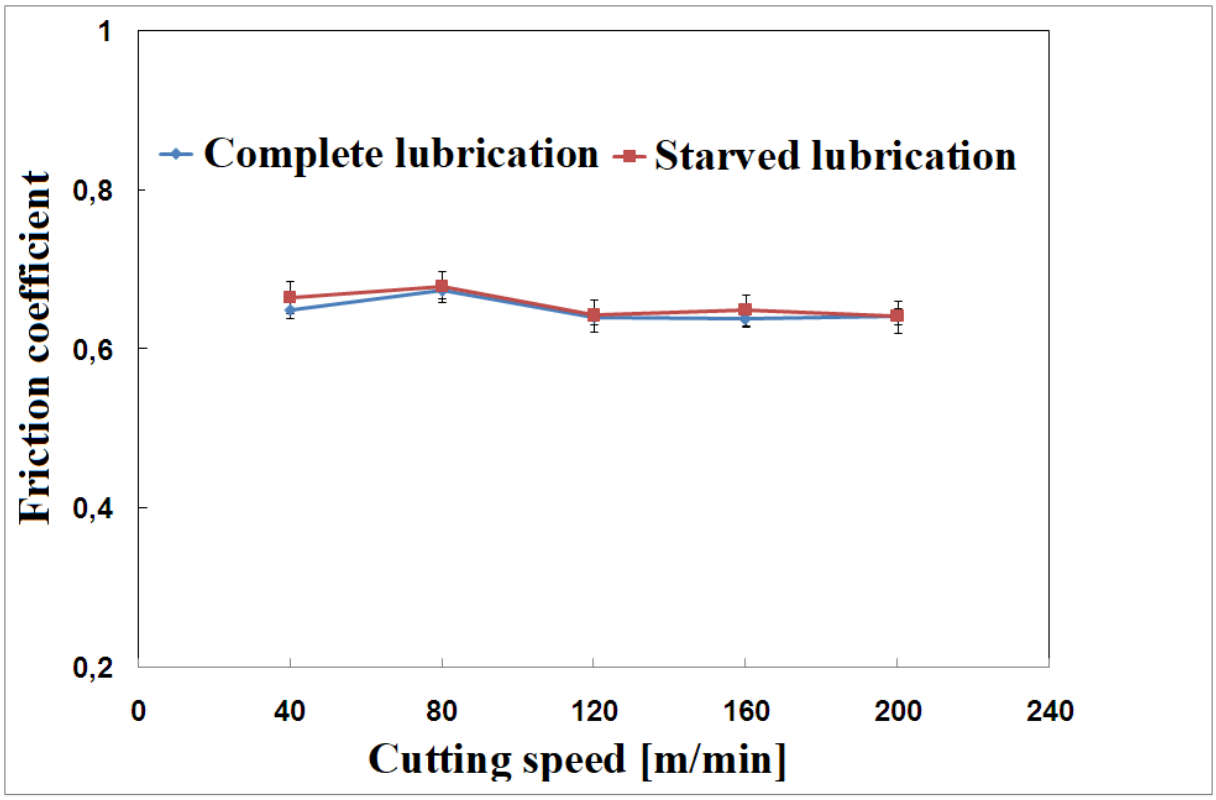

Fig.2. Friction coefficient vs. cutting speed of workpiece during machining process.

Figure 3 shows the evolution of the three components values of the cutting tools measured at different cutting speeds varying from 40 to 200 m/min. They were obtained during the turning operation carried-out under both different lubrication conditions. The cutting speed significantly affected the cutting force of the cutting inserts. The cutting behaviour of the tools decreased in both lubrication cases of the order of 7% to 10%.

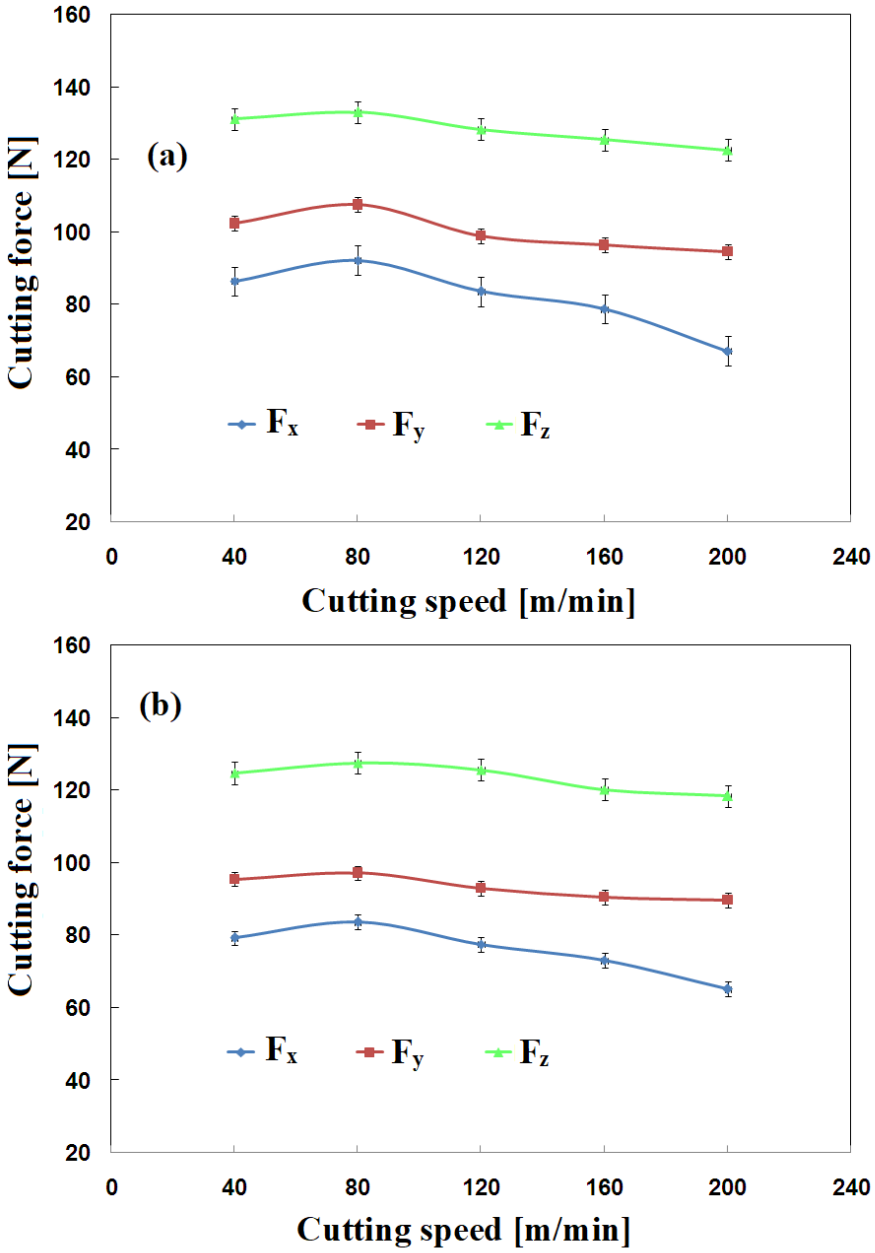

Fig.3. Evolution of cutting forces vs. cutting speeds obtained using textured cutting inserts under (a) complete fluid lubrication and (b) starved fluid lubrication.

4. FE simulation of the turning process

4.1. Material constitutive model

The constitutive model of Johnson-Cook (JC) was utilised to modelling the mechanical behaviour of the material to be machined [25]. It allows thermo-mechanical coupling to be taken into account in this process in order to correctly allowing reproducing the thermo-mechanical phenomena interconnection in the cutting area. In this FE model, the influence of strain, strain rate and temperature on yield stress were defined by three multiplicative terms.

$$\sigma = (A + B\varepsilon^{n})\left[1 + Cln\left(\frac{\dot{\varepsilon}}{\dot{\varepsilon}_0}\right)\right]\left[1 - \left(\frac{T - T_0}{T_m - T_0}\right)^{m}\right]$$

where σ was the flow stress, ε was the true strain, $\dot{\varepsilon}_0$ was the reference true strain rate, $\dot{\varepsilon}$ was the true strain rate, T_0 was the ambient temperature, T_m was the workpiece material melting temperature, T was the workpiece temperature. n was the strain hardening rate index, A was the initial yield stress, B was the hardening coefficient, C was the strain rate sensitivity coefficient, m was the temperature softening index, T_0 was the lowest experimental temperature, and T_m was the material melting temperature.

The first term of the law J-C illustrates the work hardening behaviour of the material. It consists of the parameters B and n, namely the coefficient of resistance and work hardening. The second term corresponds to the effect of the strain rate. Finally, the third term relates the temperature factor defined differently for different materials. The specific values of the parameters were shown in Table 3.

Table 3 summarizes the Johnson-Cook parameters of Ti6Al4V alloy based on α phase using in our numerical analysis.

Yield strength A [MPa]	Hardening modulus B [MPa]	Hardening coefficient n	Strain rate sensitivity C	Thermal softening coefficient m	T_{melt} [°C]	T_{room} [°C]
889.37	683.71	0.451	0.035	1	1647	21

Table 3. Johnson-Cook material constants of titanium alloy used for FE simulations.

4.2. FE Turning process simulation

Finite element analysis software LSDYNA/Explicit was used, and three-dimensional model was applied. Coupled thermomechanical analysis was used to include thermal effects.

The 3D model developed in this work simulates the orthogonal cutting of an ordinary carbon steel cylindrical part made using a coated tungsten carbide cutting insert (K10). The geometric dimensions of the cylindrical bars considered in our 3D model were 200 mm in length by 50 mm in diameter. The cutting insert geometry was taken in accordance with a CNMA 120408 type cutting insert. The relative movement between the cylindrical bar and the cutting insert was simulated by a horizontal translational movement at constant speed. It was affected on all the nodes of the cutting tool, which was assumed to be rigid and undeformable. The nodes along the left and bottom sides of the cylindrical bars were fixed. In this study, different cutting speeds varying between 40 m/min and 200 m/min were tested. The cutting-edge engagement length was 0.4 mm.

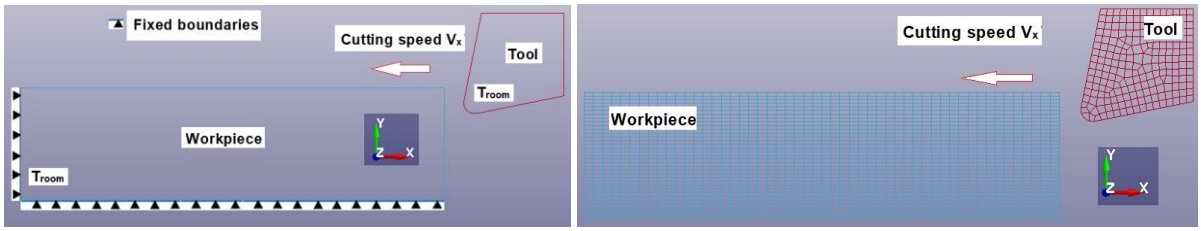

Fig.4. (a) CAD model of cutting insert and workpiece and (b) thermo-mechanical initial conditions of the cutting insert and workpiece for orthogonal cutting process.

The mechanical behaviour of the cutting inserts was considered to be thermo-elastic while the titanium alloy has been taken into account thanks to the constitutive model J-C. The cylindrical bars and the cutting tool have been described with an adaptive mesh by 28,000 and 36,000 tetrahedron-mesh elements, respectively. Coulomb friction was used to model the friction with a coefficient value defined at the cylindrical bar-cutting insert interface in agreement with Bäker et al. [6] and Calamaz et al. [2]. Figure 4 illustrates a descriptive diagram of the CAD of the initial geometry and the initial conditions and limits imposed.

An FE model has been used to predict the cutting force when machining Ti-6Al-4V alloy parts under different conditions. The cutting temperature, the friction coefficient at the tool-chip interface and the constitutive model of the material have been taken into account in the proposed FE model. A flowchart of the cutting force prediction was depicted in Fig. 5.

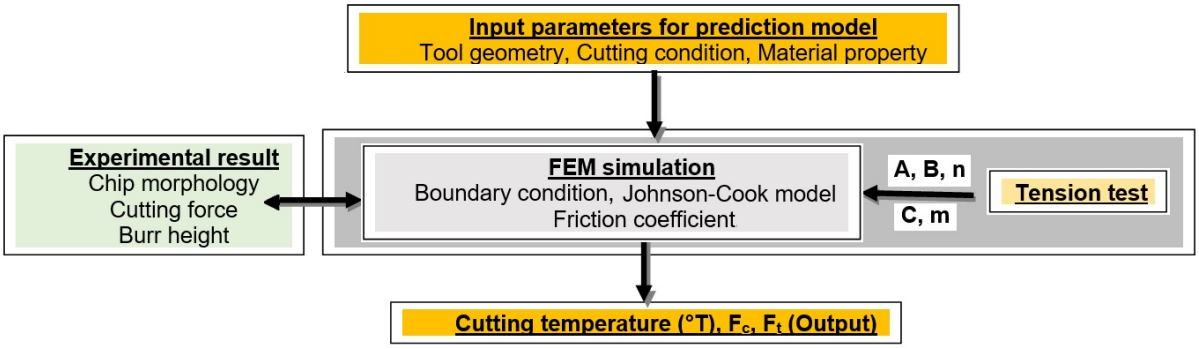

Fig. 5. Flow chart of a FE predictive cutting force model of the machining process for Ti-6Al-4V alloy.

5. Numerical simulations and discussion

5.1. Stress distribution

The Von Mises stress isovalues at a time step of 3 s were illustrated in Figure 6. The stresses were more and more distributed in the cut zone. It was clearly seen that the stress concentration zone was located near the cutting edge. The results also indicate that chips along the shear plane experience greater stresses. It was also important to numerically study the chip formation clockwork to see if the developed EF model was able to reproduce them according to the literature. Figure 7 shows the division of the shear band during the turning process, phenomenon related in the literature by Bäker et al. [6]. It has been observed that the shear was very localized in the form of a very narrow shear band which forms in two joining parts. This was because this shear band starts near the cutting edge radius of the tool and gradually spreads to the free surface of the workpiece. Then, it progresses from the free surface to the radius of the tool.

Moreover, Hou and Komanduri indicated that the cutting speed has been the important parameter for the appearance of shear bands and propose a critical cutting speed around 9 m/min above which a thermoplastic instability takes place [22]. Also, Baker et al. proposed a critical strain value close to 0.25 below which the strain hardening phenomenon may occur and above this value the Ti–6Al–4V alloy may exhibit softening [26]. This phenomenon would normally primarily promote chip segmentation during machining process by introducing an easy-slip band in the primary shear zone.

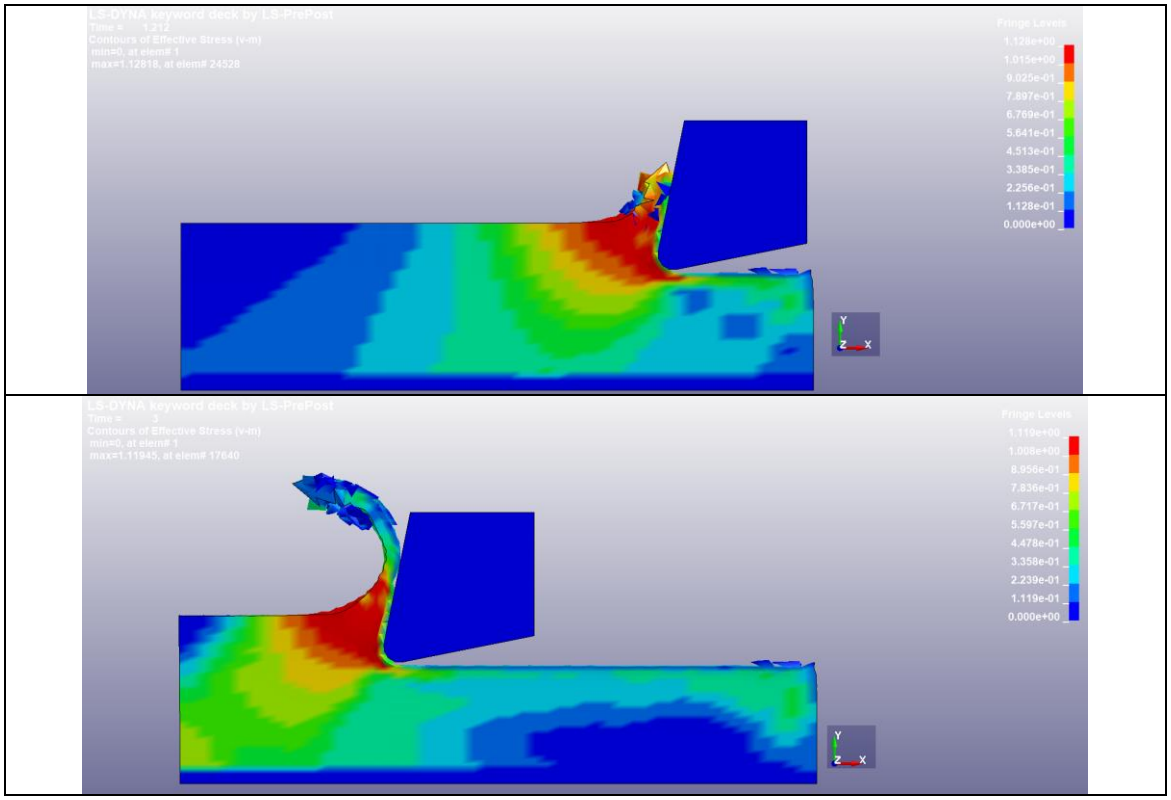

Fig.6. Von Mises stress distribution during chips formation

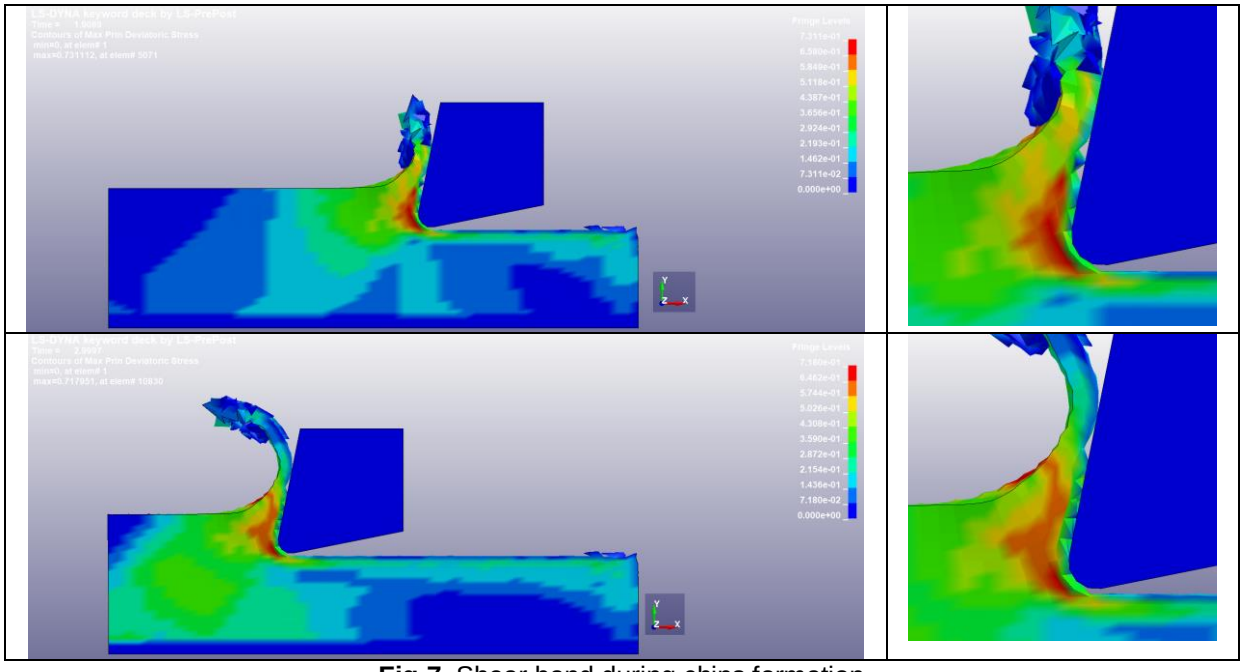

Fig.7. Shear band during chips formation.

5.2. Effects of V_c over output responses

Three cutting speed of 120 m/min, 160 m/min and 180 m/min were tested to study its influence on the final chip morphology (see Fig.8). The chip was found to be divided into two parts, one continuous and the other segmented. However, the more

the cutting speed increases, the more the chip segmentation phenomenon becomes more and more pronounced. This was due, among other things, to the effect of thermal conduction located in the shear bands. This high heating greatly influences the stiffness of the material and therefore produces a more segmented chip.

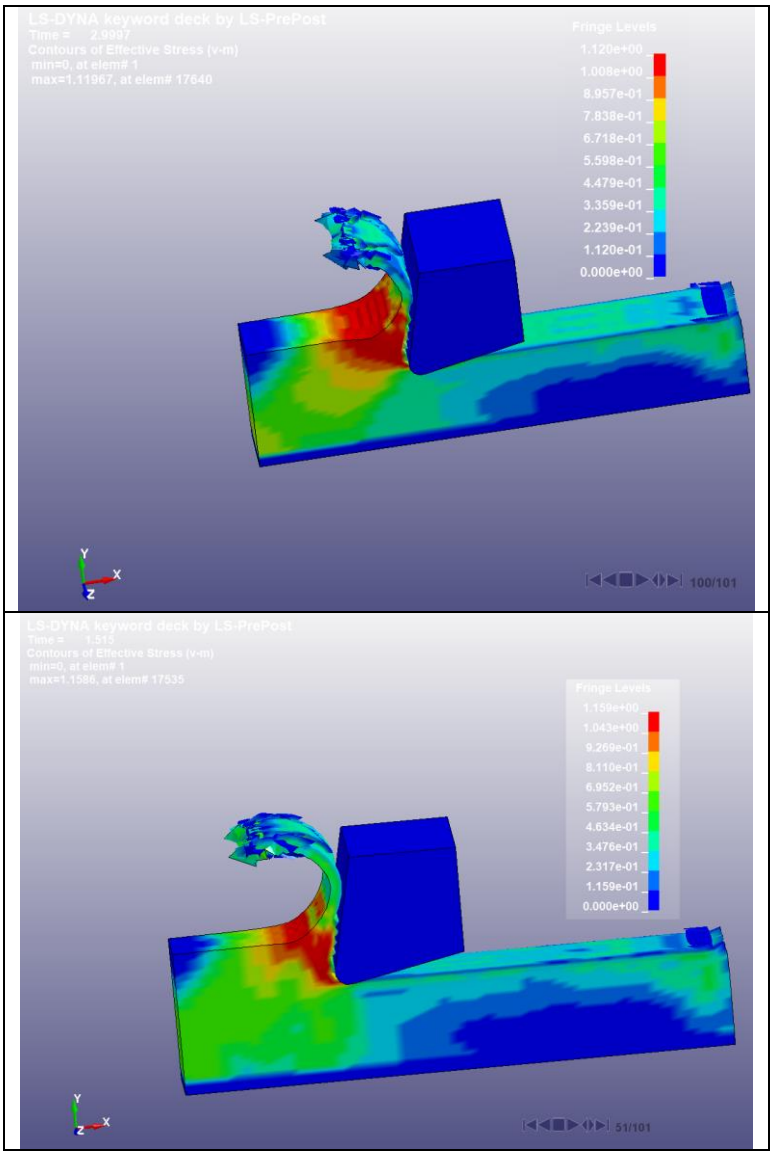

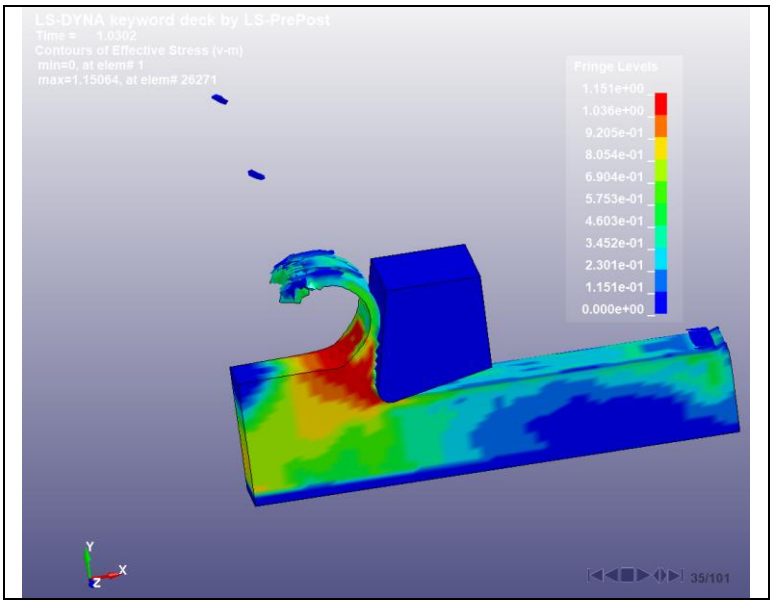

Fig.8. Effective stress distribution in chip according to cutting speed variation for starved lubrication (μ = 0.6) and f = 0.2 mm/rev: (a) V_c = 120 m/min, (b) V_c = 160 m/min and (c) V_c = 180 m/min.

5.3. Cutting temperature

During the machining, the temperature of the interaction area of the cutting tool and workpiece becomes high. Figure 9 shows the temperature field at the interface, the shear zone and the cutting face of the tool when turning a Ti-6Al-4V cylindrical bar for different cutting speeds from 120 m/min to 200 m/min. It was clearly observed that the zone at maximum temperature was mainly detected at the level of the chip-cutter wafer contact zone and near the primary shear zone. The minimum cutting temperature obtained by the EF model was approximately 680 °C at 120 m/min and it increases significantly to a maximum of 533 °C at 200 m/min, recorded at the tool interface-chip (see Fig.9). The effect of increased cutting temperature caused by higher feed rate was relatively moderate compared to that caused by higher cutting speed [11].

In addition, several studies have indicated that often high temperatures can occur during the machining operation of this type of alloy classified as difficult to machine metal [27]. The low thermal conductivity of this alloy may explain this phenomenon caused by the trapping of heat produced locally in the cutting zone, resulting in a higher turning temperature [2,5]. Many researchers have worked on temperature measurement and prediction. A review of some experimental measurement can be found in Komanduri and Hou [28].

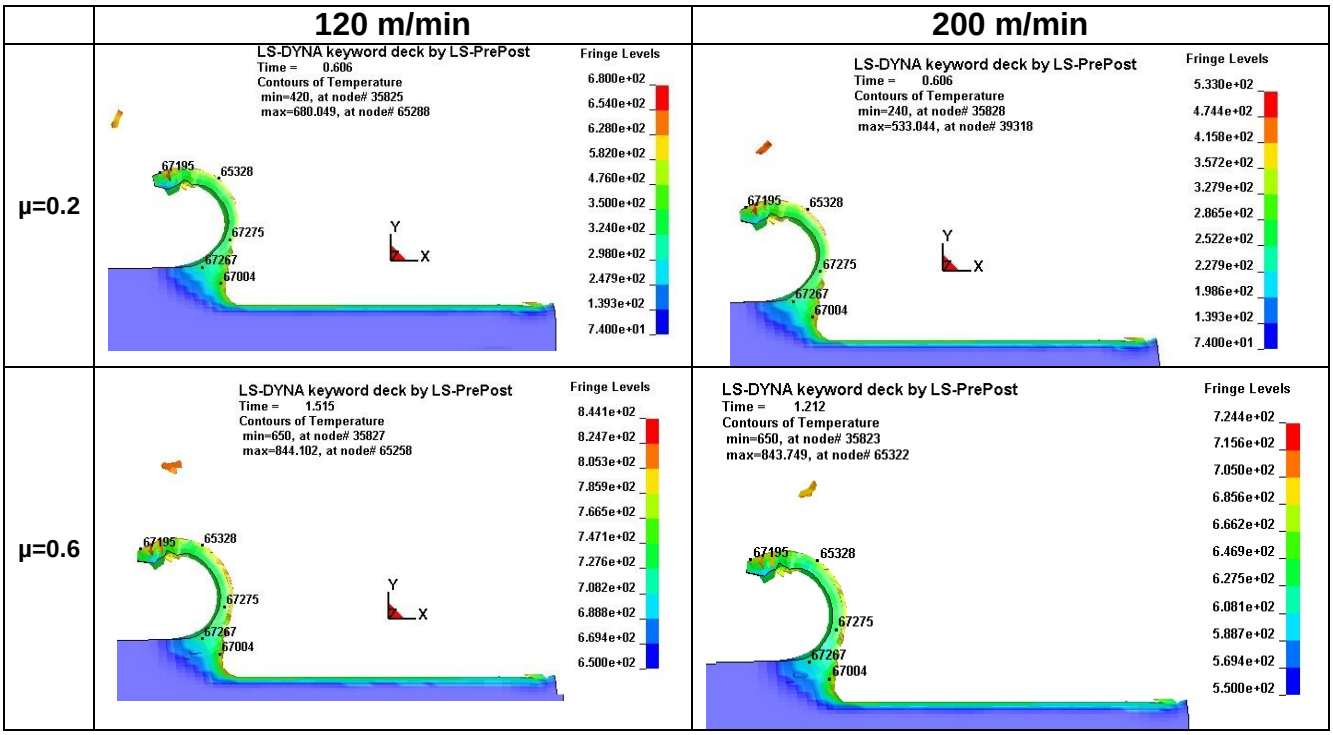

Fig.9. Temperature distribution over the cutting zones for (a) full lubrication conditions (μ=0.2), and (b) starved lubrication (μ=0.6).

5.4. Lubrication effects

To study the lubrication effect on the stress state of the Ti-6Al-4V part and the shape of the chips, friction values were taken into account, equal to 0.2 for a lubrication complete and 0.6 for severe machining at the insert cylindrical bar cutter interfaces. Figure 10 shows that there was a remarkable difference between the chips shape obtained when machining with full or severe lubrication. In machining condition with complete lubrication i.e. contact with very low friction, the final chip shape characterized by a radius of curvature at the interface of the cylindrical bar cutter insert was approximately 2, 5 lower than machining with severe lubrication. In addition, the chips thickness obtained by simulation in full lubrication was greater than that of machining with severe lubrication.

Moreover, it was interesting to indicate the weak influence of the friction coefficient on the cutting force, as it was quite clear in Fig.11. This observation was predictable because the general shape of the chip remains almost the same whatever it was. lubrication conditions, that was, the value of the friction coefficient. Calamaz et al. studied the influence of different friction models on the numerical results of Ti-6Al-4V machining simulations. They concluded that most mechanical results for the studied workpiece/tool couple were not influenced by the friction model except the temperature at the tool–chip interface [28].

Indeed, during machining, energy will be transformed in the form of heat, which causes softening at the chip/tool interface, that was to say of the contact surfaces during turning [30,31]. Similar trends were also indicated by Filice et al. [29] and Calamaz et al. [2].

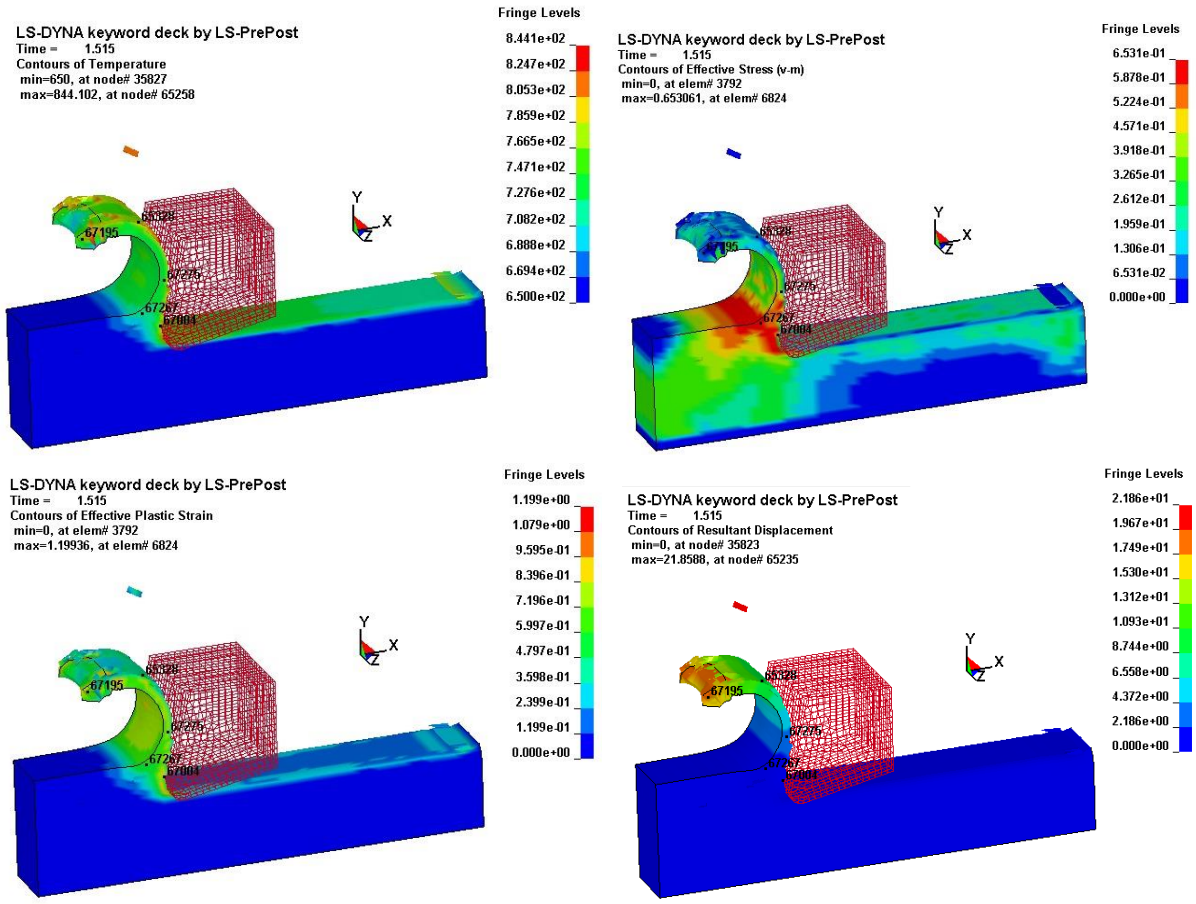

Fig.10. Numerical machining results in the cutting regions under starved lubrication conditions: (a) Temperature distributions, (b) Von-Mises stress, (c) Effective strain and (d) Resultant displacement (μ = 0.6, t =1.515 s, V_c = 200 m/min).

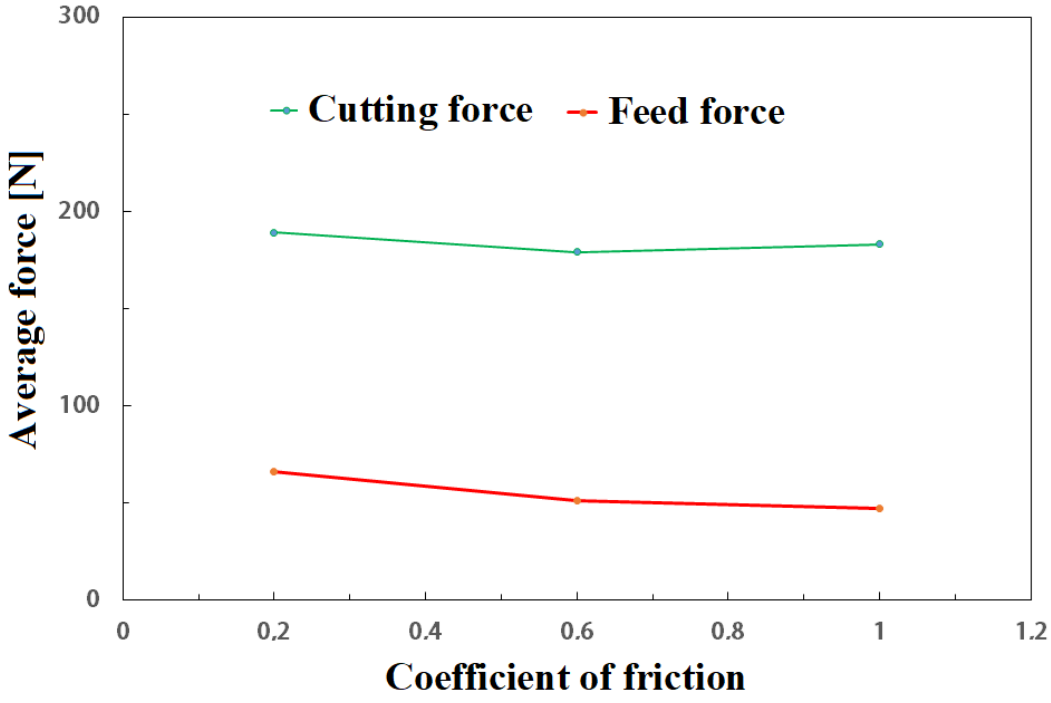

Fig.11. Evolution of the average cutting and feed forces versus coefficient of friction for f = 0.2 mm/rev, and V_c = 180 m/min.

5.5. FE model validation

Figure 12 illustrates a comparative analysis of our numerical simulations and those resulting from the experimental results during the operation of turning the titanium alloy in conditions of full or starved lubricant. The same tendency was observed for the feed forces and the thrust forces generated during cutting. They were less noticeably affected by cutting speed. This variation was estimated between 175 ± 5N whatever the lubrication conditions. Also, the friction coefficients also follow the same trend as those of the cutting forces whether for the experimental conditions as for those obtained in simulations (see Fig.13). In addition, we can see that our numerical data was slightly lower than the experimental data probably due to the complexity of the cutting conditions, the turning environment, and also due to the measurement error and vibrations not taken into account in our model. It can be concluded that the results provided by the 3D model were in good agreement under the two conditions of complete or starved lubrication with the experimental data with an error difference of only 5 to 10%.

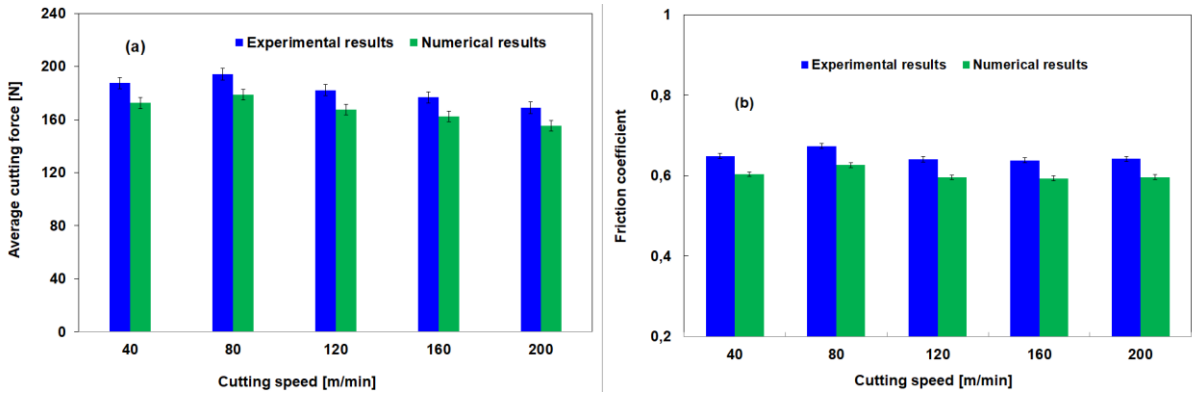

Fig.12. Comparison of experimental and simulated cutting forces under starved lubrication.

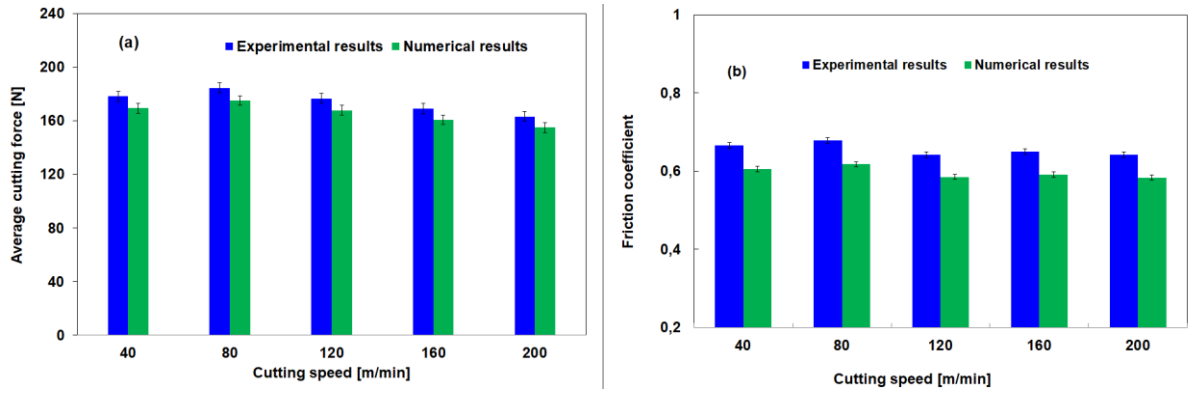

Fig.13. Comparison of experimental and simulated cutting forces under full lubrication conditions.

To complete our comparative analysis of the chip obtained and its morphology, measurements of the geometric characteristics of the chip shape were carried-out. Three morphological data were used, namely the spacing of peaks, valleys and segments. It was noted that a well agreement was observed with mean relative errors close to 10% between our numerical data and the experimental results (see Table 4).

Cutting parameters		Chip morphology [µm]					
		Peak	Valley	Spacing	Peak	Valley	Spacing
		Full lubrication			Starved lubrication		
V=80 m/min	Experiments	200	110	75	210	115	84
	Simulations	181	105	69	173	107	71
	Relative error	9.5%	4.5%	8%	17.6%	6.9%	15.5%
V=120m/min	Experiments	193	103	69	198	109	73
	Simulations	176	98	63	179	101	65
	Relative error	8.8%	4.9%	8.7%	9.6%	4.9%	7.3%
V=160 m/min	Experiments	189	101	67	193	105	70
	Simulations	172	94	62	175	97	65
	Relative error	9%	6.9%	6%	9.3%	7.6%	7.1%

Table 4. Comparative results concerning chip morphology characteristics.

Based on comparison and analysis of the chip morphology and cutting force on the simulation and experiment, the two-dimensional orthogonal cutting simulation model for Ti-6Al-4V alloy was reasonable and reliable. Thus, this model can be used to simulate and predict the actual machining process of Ti-6Al-4V alloy.

6. Conclusion

The simulations and FE experiments have clearly shown that the lubrication conditions as well as the cutting parameters lead to a marked improvement in the cutting performance of the tools and also to an increased tool life in the machining of the alloy of titanium Ti-6Al-4V. The FE simulation with the model parameters reported in this work has been well validated experimentally in the estimation of tool cutting forces in the Ti-6Al-4V titanium alloy. Other interesting findings were listed below:

- The level of equivalent plastic deformations was 5 to 7% higher for high cutting speeds leading to more wavy chips;
- Turning was accompanied by considerable heat generation in the cutting zone, affecting material properties of the treated workpiece.
- The temperature in the cutting region was about 119° under starved lubrication lower due to the elimination of friction heating;
- The drop in process temperature was recorded for numerical simulations of cutting with reduced feed; this result was in good agreement with our experimental measurements and was explained by a reduced rate of material removal.

The results revealed that the model could correctly predict the cylindrical turning step with acceptable errors. The numerical results show good agreement in the experimentally measured values of the machining experiments.

Future work will mainly focus on the final morphology of the chips formed and also on the cutting mechanism. Particular attention will be paid to the shape of the cutting tools (cutting angles....) as well as to the cutting parameters such as the feed rate, the cutting speed and the radial depth of cut. This will facilitate establishing the robustness of the proposed model and potential dependencies on various

parameters. Finally, a special attention should be paid to appropriate selection of the Johnson-Cook (J-C) constitutive parameters.

References

1. K. Palaniappan, M. Sundararaman, H. Murthy, R. Jeyaraam, B. C. Raoa , Influence of workpiece texture and strain hardening on chip formation during machining of Ti-6Al–4V alloy. Int. J. Mach. Tools and Manuf., 173 (2022), pp. 103849.

2. M. Calamaz, D. Coupard, F. Girot, A new material model for 2D numerical simulation of serrated chip formation when machining titanium alloy Ti-6Al-4V. Int J Mach Tools Manuf., 48 (2008), pp. 275-288

3. W. Zhang, C. Cheng, X. Du, X. Chen, Experiment and simulation of milling temperature field on hardened steel die with sinusoidal surface. International Journal on Interactive Design and Manufacturing (IJIDeM) 12 (2018), pp. 345-353

4. M. Lotfi, H. Ashrafi, S. Amini, Farid, M. Jahanbakhsh, Characterization of various coatings on wear suppression in turning of Inconel 625: A three-dimensional numerical simulation. Proc. Inst. Mech. Eng. Part J: J. Eng. Tribol. (2016) 1350650116677131.

5. D. Yang, Z. Liu, X. Ren, P. Zhuang, Hybrid modeling with finite element and statistical methods for residual stress prediction in peripheral milling of titanium alloy Ti-6Al-4V. Int J Mech Sci, 108–109 (2016), pp. 29-38

6. M. Bäker, J. Rosler, C. Siemers, A finite element model of high speed metal cutting with adiabatic shearing. Comput Struct, 80 (2002), pp. 495-513.

7. S Yang, X. Tong, X. Liu, Y. Zhang, C. He, Investigation on the temperature field under the action of the blunt tool edge for precision cutting of titanium alloys. International Journal on Interactive Design and Manufacturing (IJIDeM) 12 (2018), pp. 823-831

8. T. Wang, L. Xie, X. Wang, Simulation study on defect formation mechanism of the machined surface in milling of high volume fraction SiCp/Al composite. Int J Adv Manuf Technol, 79 (5-8) (2015), pp. 1185-1194.

9. J.W. Liu, K. Cheng, H. Ding, et al., Simulation study of the influence of cutting speed and tool-particle interaction location on surface formation mechanism in micromachining SiCp/Al composites. Proc Inst Mech Eng C J Mech Eng Sci, 232 (11) (2018), pp. 2044-2056.

10. A. Li, J. Zang, J. Zhao, Effect of cutting parameters and tool rake angle on the chip formation and adiabatic shear characteristics in machining Ti-6Al-4V titanium alloy. Int J Adv Manuf Technol, 107 (2020), pp. 3077-3091

11. A. Li, J. Zhao, G. Hou, Effect of cutting speed on chip formation and wear mechanisms of coated carbide tools when ultra-highspeed face milling titanium alloy Ti-6Al-4V. Adv Mech Eng 9(7) (2017) : 1687814017713704

12. G. Hou, A. Li, X. Song, H. Sun, J. Zhao, Effect of cutting parameters on surface quality in multi-step turning of Ti-6Al-4V titanium alloy. Int J Adv Manuf Technol, 98 (2018), pp. 1355-1365

13. A. Vyas, M.C. Shaw, Mechanics of saw-tooth chip formation in metal cutting, Journal of Manufacturing Science and Engineering 121 (1999), pp. 163-172.

14. J. Hua, R. Shivpuri, Prediction of chip morphology and segmentation during the machining of titanium alloys, Journal of Materials Processing Technology 150 (2004), pp. 124-133.

15. U. Umer, M. Ashfaq, J. Qudeiri, et al., Modeling machining of particle-reinforced aluminum-based metal matrix composites using cohesive zone elements. Int J Adv Manuf Technol, 78 (5-8) (2015), pp. 1171-1179.

16. D.N. Zhang, Q.Q. Shangguan, C.J. Xie, et al., A modified Johnson-Cook model of dynamic tensile behaviors for 7075-T6 aluminum alloy. J Alloys Compd, 619 (2015), pp. 186-194.

17. G. Chen, J. Caudill, C. Ren, I. S.Jawahir, Numerical modeling of Ti-6Al-4V alloy orthogonal cutting considering microstructure dependent work hardening and energy density-based failure behaviors. Int. J. Mach. Tools and Manuf., 82 (2022), pp. 750-764.

18. Y. Burhanuddin, S. Harun, G.A. Ibrahim, FEM simulation of machining AISI 1045 steel using driven rotary tool Appl. Mech. Mater. (2015), pp. 758.

19. A. Li, J. Pang, J. Zhao, J. Zang, F. Wang, FEM-simulation of machining induced surface plastic deformation and microstructural texture evolution of Ti-6Al-4V alloy. International Journal of Mechanical Sciences, Vol. 123 (2017), pp. 214-223.

20. X. Zhou, L. He, T. Zhou, H. Jiang, J. Xu, P. Tian, Z. Zou, F. Du, Multiscale research of microstructure evolution during turning Ti-6Al-4V alloy based on FE and CA, J. Alloys and Compounds, 922 (2022), pp. 166202.

21. G. Chen, C. Ren, X. Yang, X. Jin, T. Guo, Finite element simulation of high-speed machining of titanium alloy (Ti-6Al-4V) based on ductile failure model. Int J Adv Manuf Technol, 56 (2011), pp. 1027-1038

22. W. Chen, J. Xue, D. Tang, H. Chen, S. Qu, Deformation prediction and error compensation in multilayer milling processes for thin-walled parts. Int J Mach Tools Manuf, 49 (2009), pp. 859-864

23. L. Zhou, S. Huang, D. Wang, et al., Finite element and experimental studies of the cutting process of SiCp/Al composites with PCD tools. Int J Adv Manuf Technol, 52 (5-8) (2011), pp. 619-626.

24. Z. Chen, J. Zhang, P. Feng, Z. WuA simulation study on the effect of micro-textured tools during orthogonal cutting of titanium alloy Ti–6Al–4V, Appl Mech Mater, 281 (2013), pp. 389-394.

25. Johnson G, Cook W. A constitutive model and data for metals subjected to large strains, high strain rates and high temperatures. In: Proceedings of the seventh international symposium on ballistics. The Hague, The Netherlands; (1983) pp. 541-547.

26. M. Baker, J. Rösler, C. Siemers, A finite element model of high speed metal cutting with adiabatic shearing. Computers and Structures, 80 (5,6) (2002), pp. 495-513

27. D. Jianxin, W. Ze, L. Yunsong, Q. Ting, C. JiePerformance of carbide tools with textured rake-face filled with solid lubricants in dry cutting processes, Int. J. Refract. Met. Hard Mater., 30 (1) (2012), pp. 164-172.

28. M. Calamaz, D. Coupard, M. Nouari, F. Girot, A finite element model of high speed machining of TA6V titanium alloy, in: Sixth International Conference on High Speed Machining (HSM), San Sebastian, Spain, 21–22 March 2007.

29. L. Filice, D. Umbrello, S. Beccari, F. Micari, On the FE codes capability for tool temperature calculation in machining processes. Journal of Materials Processing Technology 174 (1-3) (2006), pp.286-292.

30. Z.-B. Hou, R. Komanduri, On a thermo-mechanical model of shear instability in machining. CIRP Annals, 44/1 (1995), pp. 69-73

31. R. Komanduri, Z.B. Hou, A review of the experimental techniques for the measurement of heat and temperatures generated in some manufacturing processes and tribology. Tribol. Int., 34 (2001), pp. 653-682